Experimental Evidence for Anticorrugating Effects in He-Metal Interactions at Surfaces

K. H. Rieder, G. Parschau, and B. Burg
Institut für Experimentalphysik, Freie Universität Berlin, Arnimallee 14, D-14195 Berlin-Dahlem, Germany
(Received 27 April 1993)

We show that systematic differences occur in the corrugations of the systems Ni(110)$c(2\times4)$H, and Rh(110)(1×3)H and (1×2)H, when determined from He and Ne diffraction: Whereas the hills along the H-free close-packed metal rows correspond to underlying metal atoms in all corrugations deduced from Ne diffraction, they are shifted to short bridge sites in all He-derived corrugations. This assignment is possible, as the H adatoms mark threefold hollow sites on both (110) substrates. These observations provide strong experimental support for anticorrugating effects in He-metal surface interactions as proposed by Annett and Haydock [Phys. Rev. Lett. **53**, 838 (1984)].

PACS numbers: 68.35.Bs, 68.45.−v, 79.20.Rf

He diffraction today is accepted as a well established surface structure method [1,2]. It has been successfully used in the last decade to elucidate the structures of reconstructed surfaces as well as rather complicated adatom configurations [2,3]. Ne diffraction was only recently shown to be applicable for investigations of adsorbate structures [4]. The advantages of atomic beam diffraction lie in its absolutely nondestructive nature as well as in its sensitivity to the topmost surface layer, both due to the very low particle energies ($E_i = 20$–100 meV). The information on the surface structure is provided by the corrugation function $\zeta(\underline{R})$ [$\underline{R}$ denotes a two-dimensional vector in the surface plane (x,y); z is the direction perpendicular to the surface] which can in general be obtained in a manner free of any model assumptions on the surface structure by assuming a general Fourier ansatz for $\zeta(\underline{R})$ and determining the Fourier coefficients via fitting calculated to experimental intensities for a large number of diffraction beams [1,3]. As shown by Esbjerg and Nørskov [5], $\zeta(\underline{R})$ corresponds in first order to a contour of constant surface electronic charge density $\rho(\underline{r})$ related linearly to the incoming particle energy E_i. Thus from inspection of $\zeta(\underline{R})$ the arrangement of the surface atoms can often be inferred [1–4].

Annett and Haydock [6] were the first to theoretically discuss an extension of this simple picture leading to the possibility of anticorrugating effects. According to their proposition the repulsive part of the particle-surface interaction potential should read

$$V_{\mathrm{AH}}(\underline{r}) = \alpha\rho(\underline{r}) + \beta\nabla^2\rho(\underline{r}) - \nu\rho_u(\underline{r}) . \quad (1)$$

Here, the first term denotes the Esbjerg-Nørskov leading repulsive term [5]. The second term accounting for the inhomogeneities of the electron distributions should lead to a lateral smearing of the corrugation; it should be more pronounced for Ne than for He, but was shown to be generally very small [6,7]. Most important in the present context is the third term, since it gives rise to anticorrugating effects due to the hybridization of the orbitals of the incoming atoms with the unoccupied metal states and is thus proportional to the unoccupied density of states $\rho_u(\underline{r})$. A simple physical picture of the influence of this anticorrugating term can be obtained [6,7] by observing (Fig. 1) that unoccupied states have essentially antibonding character with larger densities at top positions of the surface atoms than at bridge sites. Consequently, He (ground state $1s^2$) will be more strongly attracted at top positions due to the large overlap between the He $1s^2$ and the surface wave functions of the unoccupied states than at center positions where the overlap is zero and the corrugation will thus be diminished (Fig. 1, left side). For Ne ($2s^2 2p^6$), on the other hand, this "anticorrugating effect" is expected to be smaller, because for the $2p_x$ orbital the situation is exactly reversed as depicted on the right side of Fig. 1; thus, the Ne $2p_x$ orbital counteracts the anticorrugating influence of the Ne $2s^2$ orbital [6,7] leading to $\nu \approx 0$ for Ne in Eq. (1). For He/Ni(110) Annett and Haydock [6] have determined the value of ν semiempirically by adjusting the corrugation amplitude perpendicular to the close-packed rows (i.e., along [001]) to obtain agreement with the experimentally observed corrugation amplitude [8]. For the direction along the close-packed rows [1$\bar{1}$0], they found that the so determined anticorrugating contribution for Ni(110) leads

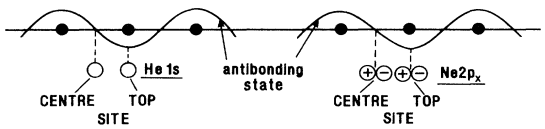

FIG. 1. Illustration of the origin of anticorrugating effects arising from the interaction of He with an unoccupied antibonding metal surface state. Left side: The He $1s^2$ orbital shows strong overlap with the unoccupied metal state at top positions, whereas the overlap is zero at bridge positions where the metal wave function changes sign; this leads to an attraction of the He atoms at the top positions and thus to a reduction of the basic corrugation which is due to the surface electron charge density [see Eq. (1)]. Right side: For Ne the $2p_x$ orbital shows no interaction with the metal state on-top sites but strong overlap at bridge sites where both p_x and metal orbitals change sign; thus in the case of Ne the $2p_x$ orbital counteracts the influence of the $2s$ orbitals leading to a much smaller anticorrugating contribution than in the case of He. Adapted from Annett, Ref. [7].

0031-9007/93/71(7)/1059(4)$06.00

even to a reversal of the corrugation, so that the corrugation maxima should correspond to short bridge sites of the close-packed rows. These results were questioned in a subsequent theoretical calculation of Harris and Zaremba [9], who employed the local density approach and found that the anticorrugating effects should be appreciably smaller. However, in response to Ref. [9], Annett and Haydock published first principle calculations [10], which supported their initial conclusions. Obviously, the situation calls for a decision on experimental grounds.

In the present paper we show that systematic differences in the corrugations of partially hydrogen covered (110) surfaces of Ni and Rh are indeed found when determined with He and Ne diffraction: Whereas in all Ne-derived corrugations the hills along the (adsorbate-free) close-packed metal rows correspond to underlying metal atoms, in all He-derived corrugations the hills correspond to short bridge sites between the metal atoms. These results are comprised in Fig. 2 and concern the three systems Ni(110)c(2×4)H, Rh(110)(1×3)H, and Rh(110)(1×2)H. These adsorption phases were chosen because (i) they exhibit close-packed metal rows, which are not covered with H adatoms, and (ii) the H locations on both surfaces are well established by quantitative low energy electron diffraction (LEED) analyses [11,12] to be the threefold coordinated sites drawn in the sphere models of Fig. 2. Furthermore, the electronic structures of Ni and Rh are very similar [13].

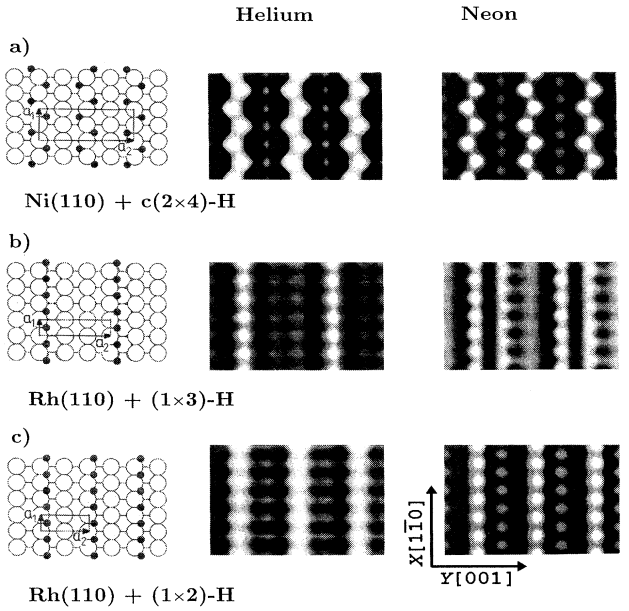

FIG. 2. Sphere models of H phases on Ni(110) and Rh(110) together with grey scale representations of the corrugation functions derived from He and Ne diffraction: (a) Ni(110)-c(2×4)H, (b) Rh(110)(1×3)H, (c) Rh(110)(1×2)H. In the sphere models open large circles denote metal atoms and full small circles H adatoms at the locations determined by LEED. The areas of the corrugations correspond to those of the sphere models. The H atoms have the largest corrugation amplitudes and thus show up as the brightest spots in the grey scale top views. Note that in all He-derived corrugations there occur less bright maxima between the H atoms along [001] on all H-free metal rows in disagreement with the true atom arrangements shown in the sphere models. In contrast to this, in the Ne-derived corrugations the metal maxima are shifted by $a_1/2$ along [1$\bar{1}$0] in agreement with the true surface structures.

It is important to emphasize that the H adatoms are needed in our analyses to mark the threefold coordinated sites, so that other areas of the corrugation can be properly assigned. The clean surfaces on principle cannot be used to connect the corrugation features with the underlying atomic geometry, as the diffraction equation [1,3]

$$\sum_{\underline{G}} A_{\underline{G}} \exp\{i[(k_{Gz}-k_{iz})\zeta(\underline{R})+\underline{G}\underline{R}]\} = -1 \qquad (2)$$

is invariant against any displacement $\underline{R} \rightarrow \underline{R}+\underline{R}'$ parallel to the surface. Equation (2) determines the scattering amplitudes $A_{\underline{G}}$ of the different reciprocal lattice vectors $\underline{G}$ for the corrugation $\zeta(\underline{R})$; k_{iz} and k_{Gz} are the components of the wave vectors of the incoming and diffracted beams perpendicular to the surface. The diffraction intensities are given by $I_{\underline{G}}=|A_{\underline{G}}|^2 k_{\underline{G}z}/k_{iz}$. The corrugation functions shown in Fig. 2 were derived by best-fit intensity analyses of several diffraction spectra measured with angles of incidence between 25° and 40° and different beam energies using Eq. (2). We here restrict a detailed discussion of the diffraction results to the system Rh(110)(1×2)H, since analogous results were obtained for all three systems investigated. The corrugation is described mathematically by writing for the metal substrate corrugation the truncated Fourier series [reference is made to the unit cell depicted in the sphere model of Fig. 2(c)]

$$\zeta_S(x,y) = (a_{10}\cos X + a_{01}\cos Y)/2 + a_{11}\cos X \cos Y, \qquad (3)$$

with $X=2\pi x/a_1$ and $Y=2\pi y/(a_2/2)$ (x along and y perpendicular to the close-packed metal rows; $a_2/2=a_{\mathrm{Rh}}=3.8$ Å, $a_1=a_{\mathrm{Rh}}/\sqrt{2}$) and by modeling the H adatoms as Gaussian hills

$$\zeta_{\mathrm{H}}(x,y) = h_{\mathrm{H}} \exp\left[-4\ln 2\left[\left(\frac{x-x_{\mathrm{H}}}{B_x}\right)^2+\left(\frac{y-y_{\mathrm{H}}}{B_y}\right)^2\right]\right], \qquad (4)$$

with h_{H} denoting the height of the H adatom hills, $x_{\mathrm{H}}, y_{\mathrm{H}}$ their lateral distances relative to the next metal atoms, and B_x, B_y their widths along x and y. In Figs. 3 and 4 we present experimental spectra (solid lines) obtained with both He and Ne. The best-fit coefficients are given in Table I. Note that x_{H} was also treated as a fit parameter and its best-fit value for both He and Ne agrees with the value $a_1/2$ in accordance with the threefold coordinated sites occupied by the H adatoms. The values of y_{H} are also in agreement with this adsorbate site (for an extended discussion of the structural conclusions based on the

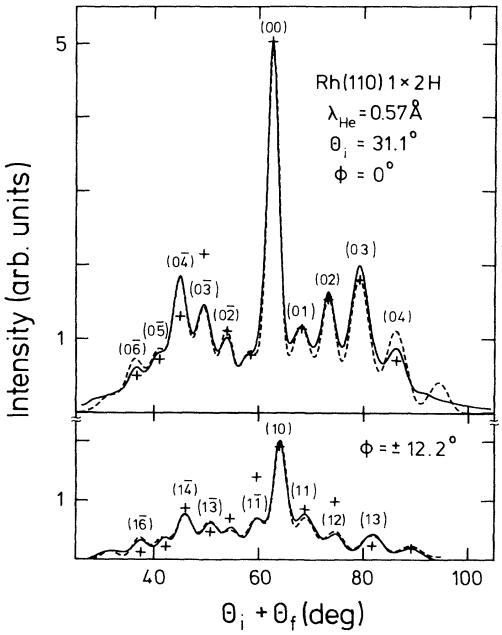

FIG. 3. Experimental He diffraction scans (solid lines) for Rh(110)(1×2)H. The dashed line indicates the intensity distribution of the best-fit result (the corresponding parameters are given in Table I). The crosses indicate the best-fit peak intensities of a corrugation, in which the metal maxima have been forced to lie above the metal atoms; the agreement is clearly worse.

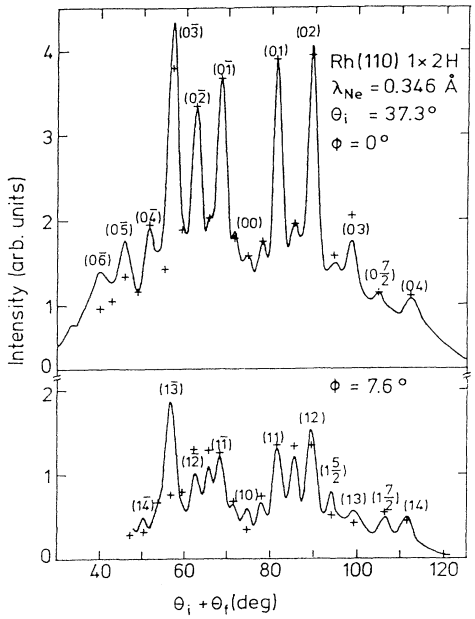

FIG. 4. Experimental Ne diffraction scans (solid lines) for Rh(110)(1×2)H. The crosses indicate the best-fit peak intensities (the corresponding parameters are given in Table I).

He-derived corrugations, see Refs. [14] and [15]). The best-fit result for the intensities is given as a dashed line in Fig. 3 and by crosses denoting the peak heights (with the experimental beam widths taken into account) in Fig. 4. It should be noted that the Ne corrugations systematically exhibit larger amplitudes of ~0.1 Å for the H adatoms and ~0.05 Å for the metal corrugations perpendicular to the close-packed rows. Most important, however, is the observation that the corrugation maxima along the H-free metal rows correspond to bridge sites in the He-derived corrugation and to the on-top sites in the Ne-derived corrugation as visualized in Fig. 2(c): Along the [001] direction the highest and thus brightest hills corresponding to the H adatoms are in line with the less high and less bright hills on the H-free metal rows in the corrugation derived from He diffraction; in contrast to this, the less bright hills are shifted by $a_1/2$ along $[1\bar{1}0]$ in the Ne-derived corrugation and are thus in correspondence with the locations of the underlying metal atoms as shown in the sphere model. The result that the maxima along the H-free metal rows correspond to short bridge sites in the He-derived corrugations and to top sites in the Ne-derived corrugations holds also for the two other adsorption systems investigated as shown in Figs. 2(a) and 2(b). The wrong location of the metal maxima in the case of the He-derived corrugation of Rh(110)+(1×2)H [Fig. 2(c)] is signaled by the minus sign obtained for the Fourier coefficient a_{10} (Table I). A refractive correction [1] was used in all calculations to account for an effective well depth D of the attractive part of the particle-surface potential; D was found to be practically negligible for He (2–3 meV) and ~8 meV for Ne. It is important to point out that in Fig. 3 the crosses refer to the peak values of an independent fit of the He data, in which the substrate corrugation was forced to exhibit the maxima at the metal top sites. The agreement with experiment is clearly worse: The intensities of the $(0\bar{4})$ and $(0\bar{3})$ beams are systematically reversed and the $(1\bar{1})$ beam is systematically too large. Similar results were obtained for spectra taken at other angles of incidence as well as for other He wavelengths. Analogous conclusions could be drawn for the two other phases shown in Figs. 2(a) and 2(b): All corrugations shown in Fig. 2 are those yielding the optimum agreement between measured and calculated intensities. With all these examples we have collected ample proof that the corrugation of the metal substrate,

TABLE I. Best-fit parameters for Rh(110)(1×2)H as determined for He and Ne diffraction. The substrate corrugation is described by the simple Fourier series, Eq. (3), and the H adatom hills by Gaussians, Eq. (4). Values are in angstroms. The corresponding corrugations are shown in Fig. 2(c).

	a_{01}	a_{10}	a_{11}	B_x	B_y	h_H	x_H	y_H
He	0.124	−0.06	0.01	2.32	1.76	0.31	1.34	0.86
Ne	0.15	0.035	0.027	1.84	1.43	0.4	1.34	0.9

which is small in comparison to that of the H hills (see Table I), influences the diffraction spectra in a sensitive manner. Thus the systematic differences between He and Ne observed for all three phases can certainly be regarded as well established.

In conclusion, we have provided strong evidence that in the case of He scattering at least along the close-packed metal rows (with corrugation amplitudes of a few 0.01 Å) anticorrugating effects [6,7,10] obviously are able to outweigh the basic corrugation due to the surface charge density [5] described by the first term in Eq. (1). Consequently, the hills along the close-packed rows correspond in all He-derived corrugations to short bridge sites rather than to top positions. For Ne, on the other hand, where anticorrugating effects are anticipated to play a much less important role [6,7,10], the corrugation hills along the close-packed metal rows indeed correspond to underlying metal atoms. In view of the adverse conclusions of Refs. [6] and [10] on the one side and of Ref. [9] on the other concerning the magnitude of the anticorrugating term in Eq. (1), our results certainly should stimulate further theoretical investigations on the subtleties of the interaction of the light noble gases with surfaces. In any case, adopting a pragmatic point of view, it appears safe to state that corrugations derived from Ne diffraction deliver more faithful pictures of surface atom arrangements than corrugations deduced from He diffraction; moreover, Ne "sees" larger corrugation amplitudes and may thus be more sensitive to structural details. Thus, although Ne diffraction spectra are more difficult to measure and to evaluate, Ne diffraction will certainly play an important role in the future.

The authors acknowledge partial support by the Deutsche Forschungsgemeinschaft (Sonderforschungsbereiche 6 and 290) and thank Dr. R. Koch for a critical reading of the manuscript.

[1] T. Engel and K. H. Rieder, in *Structural Studies of Surfaces with Atomic and Molecular Beam Diffraction*, edited by G. Höhler and E. A. Niekisch, Springer Tracts in Modern Physics Vol. 91 (Springer, Berlin, 1982), p. 55.

[2] K. Kern and G. Comsa, in *Molecule Surface Interactions*, edited by K. Lawley, Advances in Chemical Physics (Wiley, New York, 1989), p. 211.

[3] K. H. Rieder, in *Helium Atom Scattering from Surfaces*, edited by E. Hulpke, Springer Series in Surface Science Vol. 27 (Springer, Berlin, 1992), p. 41.

[4] G. Parschau, Doctoral thesis, Freie Universität Berlin, 1992; G. Parschau, B. Burg, and K. H. Rieder (to be published).

[5] N. Esbjerg and J. K. Nørskov, Phys. Rev. Lett. **45**, 807 (1980).

[6] J. F. Annett and R. Haydock, Phys. Rev. Lett. **53**, 838 (1984).

[7] J. F. Annett, Doctoral thesis, University of Cambridge, 1985.

[8] K. H. Rieder and N. Garcia, Phys. Rev. Lett. **49**, 43 (1982).

[9] J. Harris and E. Zaremba, Phys. Rev. Lett. **55**, 1940 (1985).

[10] J. F. Annett and R. Haydock, Phys. Rev. B **34**, 6860 (1986).

[11] W. Reimer, V. Penka, M. Skottke, R. J. Behm, G. Ertl, and W. Moritz, Surf. Sci. **186**, 45 (1987).

[12] W. Puchta, W. Nichtl, W. Oed, N. Bickel, H. Heinz, and K. Müller, Phys. Rev. B **39**, 1020 (1989).

[13] V. L. Moruzzi, J. F. Janak, and A. R. Williams, *Calculated Electronic Properties of Metals* (Pergamon, New York, 1992).

[14] G. Parschau, E. Kirsten, and K. H. Rieder, Surf. Sci. **225**, 367 (1990); Phys. Rev. B **43**, 12126 (1991).

[15] K. H. Rieder and W. Stocker, Surf. Sci. **169**, 55 (1985).

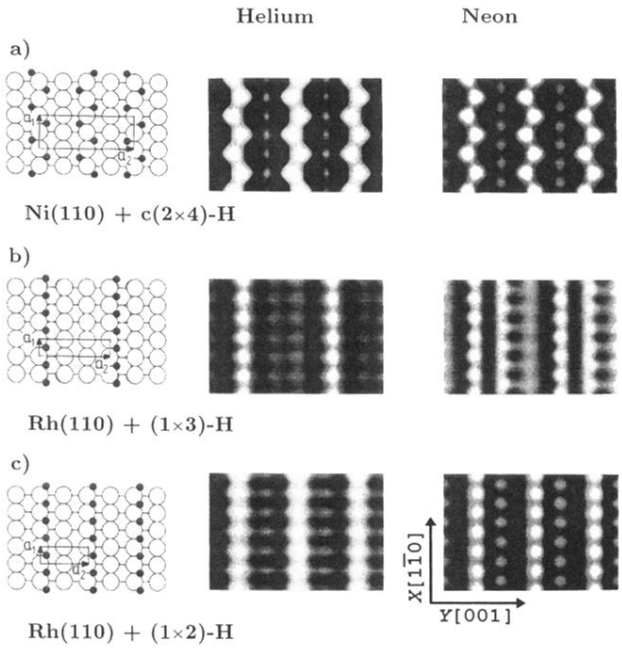

FIG. 2. Sphere models of H phases on Ni(110) and Rh(110) together with grey scale representations of the corrugation functions derived from He and Ne diffraction: (a) Ni(110)-$c(2\times4)$H, (b) Rh(110)(1×3)H, (c) Rh(110)(1×2)H. In the sphere models open large circles denote metal atoms and full small circles H adatoms at the locations determined by LEED. The areas of the corrugations correspond to those of the sphere models. The H atoms have the largest corrugation amplitudes and thus show up as the brightest spots in the grey scale top views. Note that in all He-derived corrugations there occur less bright maxima between the H atoms along [001] on all H-free metal rows in disagreement with the true atom arrangements shown in the sphere models. In contrast to this, in the Ne-derived corrugations the metal maxima are shifted by $a_1/2$ along [1$\bar{1}$0] in agreement with the true surface structures.